Development of Finger-Shaped Tactile Sensor Using Hemispherical Optical Waveguide

Hitoshi MAEKAWA*, Kazuo TANIE*, Makoto KANEKO**, Natsuo SUZUKI***, Chiyoharu HORIGUCHI**** and Takeo SUGAWARA****

A finger-shaped tactile sensor that uses an optical waveguide to detect the contact location and the surface normal of the contacted object has been developed. The hemispherical optical waveguide is covered with an elastic cover, and LEDs are installed for the light source on the edge of the waveguide. A fiber optics plate (FOP), consisting of high-density bundled optical fibers and a position sensitive detector (PSD) is used for the image guide and the optical detector. The injected light from the LEDs into the waveguide maintains total internal reflection at the surface of the waveguide and is enclosed within it. When an object contacts the sensor, the cover depresses and touches the waveguide. At that moment, scattered light occurs at the contact location due to the change of the reflection condition. The scattered light reaches the PSD through the FOP and the position of the optical input is converted to an electric signal. Processing this signal detects the contact location and the surface normal of the contacted object.

The principle and the integrated structure of the developed tactile sensor and the signal processing are described. The accuracy of the contact detection for static contact and the dynamic response for the intermittent contact of the tactile sensor are also experimentally evaluated.

Key Words: tactile sensing, finger-shaped tactile sensor, optical waveguide

1. Introduction

In recent years, investigations on multifingered robotic hands have been increasing in attempts to achieve dexterity on par with the human hand. To achieve successful grasp and manipulation of an object with a multifingered hand, the fingers must produce appropriate force-moment to restore the object to the desired position-orientation when the object is disturbed by an external force [4][7][9]. To determine such fingertip forces correctly, the contact locations of the fingertip and the object are needed since the magnitude and direction of the resultant moment exerted by the fingertip forces depend on the locations of the contact.

On the other hand, a successful grasp requires that undesired slipping or loss of contact at the fingertip should be avoided. To satisfy this, the fingertip force needs to be directed inside the friction cone where the tip is at the contact location and the axis coincides with the surface normal of the object at contact [4]. This means that information on surface normal of the object at contact is also needed to determine the appropriate fingertip force that maintains firm contact.

However, such information necessary for grasp and manipulation control is not always available when the geometrical shape or position-orientation of the grasped object is unknown. Thus, the purpose of this study is a development of a finger-shaped tactile sensor that is capable of detecting the contact location and the surface normal of the contacted object.

In other research on tactile sensing, several types of tactile sensors have already been proposed, such as use of resistive conductive rubbers [8], static capacitance [3], piezoelectric materials [2][5] or magnetoresistive devices [11]. But because of the difficulties in manufacturing such sensors in 3D shapes, they are usually configured in planar or cylindrical shapes. In addition, the surface of such tactile sensors consists of an array of discrete sensing elements with wired electrical outputs. With such a discrete sensor structure, the number of sensing elements and wires must be increased greatly when a large sensing area or high resolution is required.

In previous research, the authors proposed and investigated a planar tactile sensor using an optical waveguide to detect the profile of the contacted object [10]. In a modification of this sensor, a finger-shaped tactile sensor that can detect the contact location and surface normal of the object was developed and its capabilities experimentally evaluated [6]. The size of the previous sensor was not small enough to be compatible with the robotic hand. Also the signal processing was too time-consuming for practical application.

* National Institute of Advanced Industrial Science and Technology
** Faculty of Engineering, Hiroshima University
*** Faculty of Engineering, Tamagawa University
**** Hamamatsu Photonics K. K.

In this paper, the principle and miniaturization of the finger-shaped tactile sensor is first introduced, followed by the signal processing algorithm that determines the contact location and the surface normal of the object at the contact. Finally, the capability of the developed tactile sensor for detecting the contact in static and dynamic conditions is experimentally evaluated.

2. Principles of tactile sensor

To describe the principle of the tactile sensor, we show the structure of the previously developed scaled-up sensor [6] in Fig. 1. The optical waveguide is a hemispherical shell of glass and the light induced from the light source through the optical fibers is injected into the waveguide at its edge. Most of the injected light is totally reflected internally at the surface of the waveguide and is enclosed inside it. This is because the angle of incidence with the waveguide's surface is smaller than the critical angle determined by the refractive indices of the glass and the air.

The waveguide is covered with an elastic cover with an appropriate clearance from the waveguide. When an object contacts the cover, the cover is depressed and part of it makes contact with the waveguide. At this time, the light enclosed in the waveguide scatters at the contact location because the total internal reflection is no longer satisfied there.

The scattered light occurring at the contact location is observed by a CCD camera and its output is stored in a computer. The location of the scattered light on the CCD is measured by the image processing software. Using the geometries of the waveguide and the CCD, we can determine the contact location of the object on the sensor.

Additionally, assuming the object to be a rigid body providing enough smoothness compared with the size of the sensor, the surface normal of the object coincides with that of the sensor at the contact location. Since the geometrical shape of the sensor is known, the surface normal of the object is determined from the contact location. As a result, both the contact location and the surface normal of the object can be obtained from the location of the scattered light.

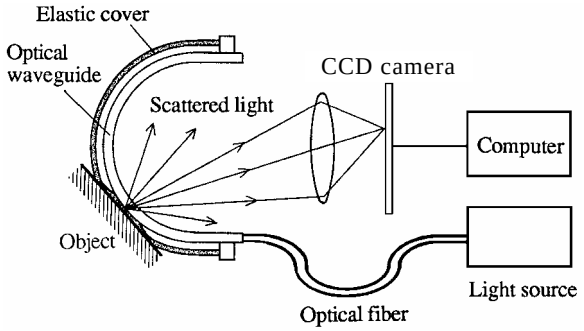

Fig. 1 Principle of finger-shaped tactile sensor

3. Requirements of tactile sensor for practical application

To apply the tactile sensor shown in Fig. 1 at the fingertip of a robotic hand for practical grasp-manipulation control, miniaturization of the sensor and faster signal processing are required. Satisfying these requirements requires integrating the sensor components in a compact size.

This has been already investigated by Begej while developing a finger-shaped tactile sensor that could acquire the local profile of a contacted object [1]. In this tactile sensor, the light led from the light source through fibers is injected into the hemispherical waveguide as in Fig. 1. The bundle of optical fibers is allocated so that their ends face to the inner surface of the waveguide and lead the scattered light occurring at the contact location from the sensor to external image detector.

In this configuration, it is possible to miniaturize the sensor by separating it from the external light source and image detector connected by optical fibers. However, since the fiber bundle is frequently bent when the sensor is implemented on the robotic hand, problems concerning the flexibility and durability of the fiber arise.

Additionally, it is difficult to realize high spatial resolution for tactile sensing at entire surface of the sensor because the number of the optical fibers arranged at each sensing point is limited. In Begej's tactile sensor, 256 optical fibers are used and the minimum spatial resolution is 0.635mm. However, this resolution is only achieved at a limited (7.62mm×7.62mm) part of the sensor surface.

To resolve such problems and miniaturize the sensor structure, a finger-shaped tactile sensor that integrates the light source, optical system and optical detector is proposed and evaluated.

4. Structure of finger-shaped tactile sensor

Figure 2 shows an overall view and the interior structure of the miniaturized tactile sensor. As in the scaled-up sensor shown in Fig. 1, the miniaturized sensor also contains a hemispherical optical waveguide (glass, outer diameter: 30mm, thickness: 2mm) and a white elastic cover (silicone rubber, outer diameter: 32mm, thickness: 1mm). Instead of an external light source with optical fibers as used in the scaled-up sensor, eight infrared LEDs are placed directly at the edge of the waveguide. The light wavelength (890nm) is selected to match the sensitive wavelength of the detector. The interference of external light coming from outside the sensor can be reduced by increasing the intensity of the light source. For this reason, more than the rated current is supplied to

the LEDs and it is intermittently modulated to prevent thermal breakdown (frequency: 5kHz, on time: 10μs, duty ratio: 1/20).

To detect light scattering at the contact location, a position sensitive detector (PSD) is used instead of a CCD camera. The PSD can convert the location of the centroid of the light intensity on its surface to four electric signals. Using the PSD, precise and fast detection (spatial resolution: 6μm, detection area: 12mm×12mm, response time: 0.5μs) is feasible. Since the outputs of the PSD are the current signal, it is converted to the voltage signal by the amplifiers integrated in the sensor.

Integrating the optical waveguide and the PSD requires a compact optical system that can transmit the scattered light from the waveguide to the PSD. Additionally, the view angle of the optical system should be as wide as possible to expand the sensing area and minimize the distance between the waveguide and the PSD. To realize such an optical system, we employed a fiber optics plate (FOP) which is a squeezed bundle of fine optical fibers capable of transmitting an image from one end to the other without distortion. One end of the FOP is hemispherically shaped to fit the inner surface of the waveguide and the other end is plane shaped to fit the PSD. The scattered light occurring at the contact of the waveguide and the cover is led to the PSD through the FOP.

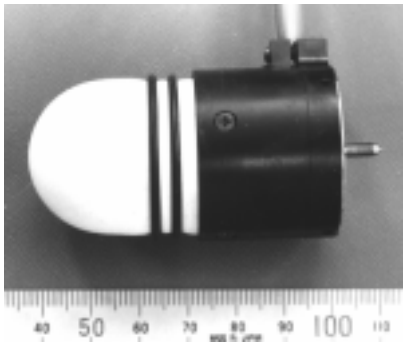

(a) Overall view

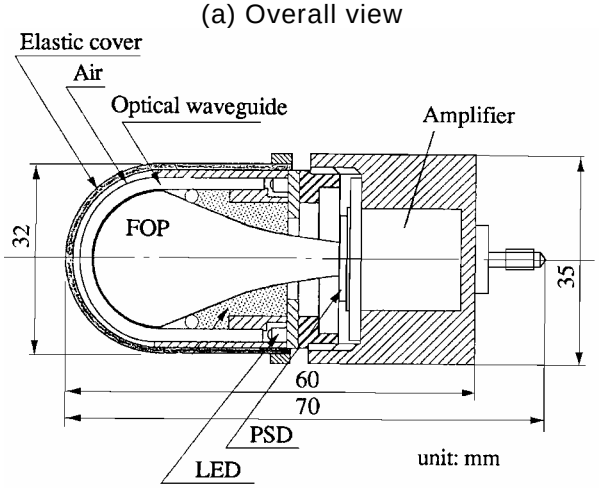

(b) Interior structure

Fig. 2 Miniaturized tactile sensor

Since the PSD is smaller than the waveguide, the FOP is tapered so the fibers are thinner as they lead from the waveguide to the PSD. Using the PSD instead of a CCD makes the forming of the FOP much easier. Since fabricating a larger PSD is much easier than a CCD, it is possible to provide a detector as large as the waveguide. Therefore, the difference between the size of both ends of the FOP is reduced and the difficulty in forming the FOP with a tapered shape is reduced.

As a result of the above miniaturizations, a tactile sensor was developed with a diameter of 32mm at the fingertip, a length of 60mm (without the thread for mechanical interface with the finger) and a weight of 100g without the cable.

5. Signal processing of tactile sensor

Figure 3 shows the signal processing of the developed tactile sensor for measuring the contact location and surface normal of the object. The PSD provides four outputs buffered by the built-in amplifiers. Since the LEDs are lit intermittently, the outputs of the PSD are modulated by the drive pulse of the LEDs. Thus, valid outputs are captured synchronously with the activation of the LEDs by a sample/hold device. The captured signals v_{x1}, v_{y1}, v_{x2} and v_{y2} are stored in the computer (CPU: i386-25MHz) through an analog-digital converter.

The first stage in signal processing is cancellation of external light noise from outside the sensor. Prior to sensing, the outputs of the PSD without an object in contact are stored as an offset. By removing the offset from the outputs of the PSD, the net PSD

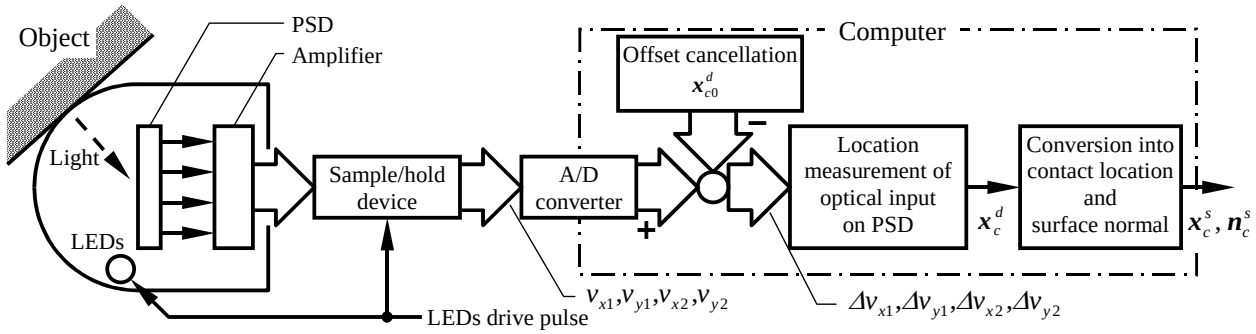

Fig. 3 Signal processing of tactile sensor

outputs Δv_{x1}, Δv_{y1}, Δv_{x2} and Δv_{y2} at contact are obtained.

Next, the location of the optical input on the PSD is determined. For formulation, the detection coordinate system o^d-$x^d y^d$ with its origin at the center of the PSD is defined as shown in Fig. 4. The location of the optical input on the PSD $\boldsymbol{x}_c^d \in \Re^2$ in this detection coordinate system is then determined as:

$$\boldsymbol{x}_c^d = \frac{L_d}{2} \frac{\begin{bmatrix} -\Delta v_{x1} + \Delta v_{y1} + \Delta v_{x2} - \Delta v_{y2} \\ -\Delta v_{x1} - \Delta v_{y1} + \Delta v_{x2} + \Delta v_{y2} \end{bmatrix}}{\Delta v_{x1} + \Delta v_{y1} + \Delta v_{x2} + \Delta v_{y2}} - \boldsymbol{x}_{c0}^d \qquad (1)$$

where L_d is the width of the PSD. In practical tactile sensing, the scattered light at the contact location spreads, which is not a point light source. In such a case, due to the characteristics of the PSD, the location of the centroid of the scattered light is determined.

The denominator of Eq. (1), namely the total of the four PSD outputs, corresponds to the intensity of the optical input. When this value is smaller than a specified threshold level, we determine that the light is not scattered at the waveguide and there is no contact on the sensor.

In Eq. (1), $\boldsymbol{x}_{c0}^d \in \Re^2$ is an experimentally determined offset which compensates for misalignment of the PSD in the sensor. When the object is contacted at the pole of the sensor, the offset $\boldsymbol{x}_{c0}^d$ is determined from the outputs of the PSD Δv_{x1}^*, Δv_{y1}^*, Δv_{x2}^* and Δv_{y2}^* so that the location of the optical input $\boldsymbol{x}_c^d$ is zero as:

$$\boldsymbol{x}_{c0}^d = \frac{L_d}{2} \frac{\begin{bmatrix} -\Delta v_{x1}^* + \Delta v_{y1}^* + \Delta v_{x2}^* - \Delta v_{y2}^* \\ -\Delta v_{x1}^* - \Delta v_{y1}^* + \Delta v_{x2}^* + \Delta v_{y2}^* \end{bmatrix}}{\Delta v_{x1}^* + \Delta v_{y1}^* + \Delta v_{x2}^* + \Delta v_{y2}^*} \qquad (2)$$

Finally, the location of the contact and surface normal of the object at the contact are determined. As shown in Fig. 4, the surface of the sensor is represented as a hemisphere with radius R_s. A polar coordinate system o^s-$\phi^s\theta^s$ and an orthogonal coordinate system o^s-$x^s y^s z^s$ sharing a common origin at the center of the hemisphere are defined as the sensor coordinate system. In these coordinate systems, the z^s axis is fixed along the line connecting the pole and the center of the hemisphere. The x^s and y^s axes are defined to be parallel to the x^d, y^d axis of the detection coordinate system respectively. At the pole of the sensor, let θ^s be zero. Also let the points that satisfy $\phi^s = 0$ or $\phi^s = \pi$ be on $x^s z^s$ plane. According to above definition, the contact location on the sensor is represented by two angles ϕ_c^s, θ_c^s ($\theta_c^s \geq 0$) regarding the polar coordinate system o^s-$\phi^s\theta^s$, and $\boldsymbol{x}_c^s \in \Re^3$ regarding the orthogonal coordinate system o^s-$x^s y^s z^s$.

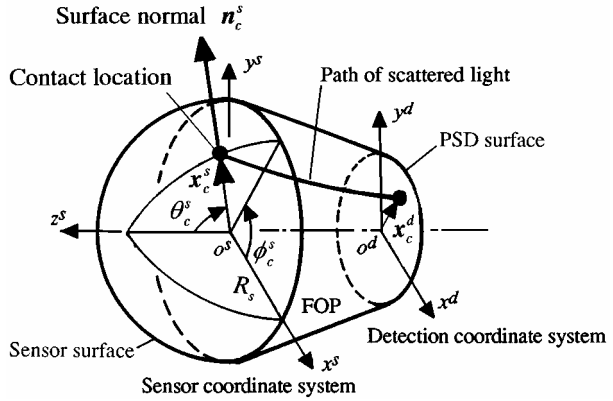

Fig. 4 Coordinate systems in tactile sensor

Suppose that a contact point ϕ_c^s, θ_c^s in the sensor coordinate system corresponds to a point $\boldsymbol{x}_c^d$ in the detection coordinate system. If the FOP guides the images from the waveguide to the PSD without distortion, the two points on the sensor surface and the PSD surface, which are optically coupled by the FOP, are related as follows:

$$\begin{bmatrix} \phi_c^s & \theta_c^s \end{bmatrix}^T = \boldsymbol{f}^s(\boldsymbol{x}_c^d) \qquad (3)$$

$$\boldsymbol{f}^s\left(\begin{bmatrix} x_{cx}^d & x_{cy}^d \end{bmatrix}^T\right) = \begin{bmatrix} \tan^{-1}\left(\dfrac{x_{cy}^d}{x_{cx}^d}\right) \\ \beta_c \sqrt{{x_{cx}^d}^2 + {x_{cy}^d}^2} \end{bmatrix} \qquad (4)$$

where β_c is a parameter converting the distance on the PSD to that on the sensor. This was experimentally determined from the location of the optical input on the PSD $\boldsymbol{x}_c^{d**}$ detected by Eq. (1) while the object is contacting the sensor at location θ_c^{s**} as:

$$\beta_c = \frac{\theta_c^{s**}}{\left|\boldsymbol{x}_c^{d**}\right|} \qquad (5)$$

Once ϕ_c^s, θ_c^s are obtained by Eqs. (3)-(4), the contact location $\boldsymbol{x}_c^s$ represented in the orthogonal coordinate system is determined as follows:

$$\boldsymbol{x}_c^s = R_s \boldsymbol{n}^s(\phi_c^s, \theta_c^s) \qquad (6)$$

$$\boldsymbol{n}^s(\phi_c^s, \theta_c^s) = \begin{bmatrix} \cos\phi_c^s \sin\theta_c^s & \sin\phi_c^s \sin\theta_c^s & \cos\theta_c^s \end{bmatrix}^T \qquad (7)$$

Since the object and the sensor share a common surface normal at the contact location, the surface normal of the object $\boldsymbol{n}_c^s \in \Re^3$ is determined as a unit vector directed from the center of the hemisphere to the contact location as:

$$\boldsymbol{n}_c^s = \boldsymbol{n}^s(\phi_c^s, \theta_c^s) \tag{8}$$

By applying the algorithm described by Eqs. (1)-(8), we determine the contact location and the surface normal of the object. In our developed sensor, the processing time and the maximum sensing rate are about 1.5ms and 670Hz, respectively.

6. Experimental evaluation of finger-shaped tactile sensor

6.1 Evaluation indexes

To evaluate the accuracy of the developed tactile sensor for measuring the contact location, two indexes, namely the error angle and the mean deviation, were defined. In the experimental evaluation, the object contacts the sensor at the specified location $\hat{P}_c$ represented by $\hat{\phi}_c^s$, $\hat{\theta}_c^s$ as shown in Fig. 5. The location of the optical input $\boldsymbol{x}_{cn}^d \in \Re^2$ $(1 \le n \le N_s)$ is measured for N_s times on the PSD while in contact. Then the mean location of measured locations $\bar{\boldsymbol{x}}_c^d \in \Re^2$ is derived as:

$$\bar{\boldsymbol{x}}_c^d = \frac{\sum_{n=1}^{N_s} \boldsymbol{x}_{cn}^d}{N_s} \tag{9}$$

Locations P_{cn} and $\bar{P}_c$ on the sensor surface corresponding to the measured locations $\boldsymbol{x}_{cn}^d$ and their mean location $\bar{\boldsymbol{x}}_c^d$ on the PSD are represented by ϕ_{cn}^s, θ_{cn}^s and $\bar{\phi}_c^s$, $\bar{\theta}_c^s$ respectively according to Eqs. (3)-(4) as:

$$\begin{bmatrix}\phi_{cn}^s & \theta_{cn}^s\end{bmatrix}^T = \boldsymbol{f}^s(\boldsymbol{x}_{cn}^d) \tag{10}$$

$$\begin{bmatrix}\bar{\phi}_c^s & \bar{\theta}_c^s\end{bmatrix}^T = \boldsymbol{f}^s(\bar{\boldsymbol{x}}_c^d) \tag{11}$$

An error angle is defined to evaluate nonlinearity when measuring the contact location. As illustrated in Fig. 5, the error angle δ_c^s is an angle between the specified contact location $\hat{P}_c$ and the mean measured contact location $\bar{P}_c$ around the center of the hemispherical sensor as:

$$\delta_c^s = \cos^{-1}\left[\boldsymbol{n}^s(\hat{\phi}_c^s, \hat{\theta}_c^s) \cdot \boldsymbol{n}^s(\bar{\phi}_c^s, \bar{\theta}_c^s)\right] \tag{12}$$

The other index for evaluating repeatable accuracy is a mean deviation representing the variance of the measured contact location. To derive the mean deviation, the deviation angle ε_{cn}^s for each measured location P_{cn} around the mean location $\bar{P}_c$ is obtained as:

$$\varepsilon_{cn}^s = \cos^{-1}\left[\boldsymbol{n}^s(\phi_{cn}^s, \theta_{cn}^s) \cdot \boldsymbol{n}^s(\bar{\phi}_c^s, \bar{\theta}_c^s)\right] \tag{13}$$

The mean deviation $\bar{\varepsilon}_c^s$ is defined as a mean value of the deviation angle for all measurements as:

$$\bar{\varepsilon}_c^s = \frac{\sum_{n=1}^{N_s} \varepsilon_{cn}^s}{N_s} \tag{14}$$

6.2 Evaluation of tactile sensor for static contact

Using the indexes previously defined, the accuracy of the developed tactile sensor for measuring the location of static contact was experimentally evaluated. The tactile sensor was fixed in the goniometer shown in Fig. 6 which provides rotational degrees of freedom along the ϕ^s and θ^s axes of the sensor coordinate system. The flat end of a rigid rod set on the goniometer contacts specified locations on the sensor. Prior to the experiments, parameters necessary for signal processing were determined by Eqs. (2), (5). The rod contacts the sensor surface at 25 specified locations and the contact location is measured by the sensor 20 times (N_s=20) for each contact. From these measurements, the measured contact location, mean measured contact location, the error angle and the mean deviation are derived.

Figure 7 shows the experimental results where the specified contact locations $\hat{P}_c$ are represented by □ and the mean measured contact locations $\bar{P}_c$ by ● in the $\phi^s\theta^s$ polar coordinate system. It was

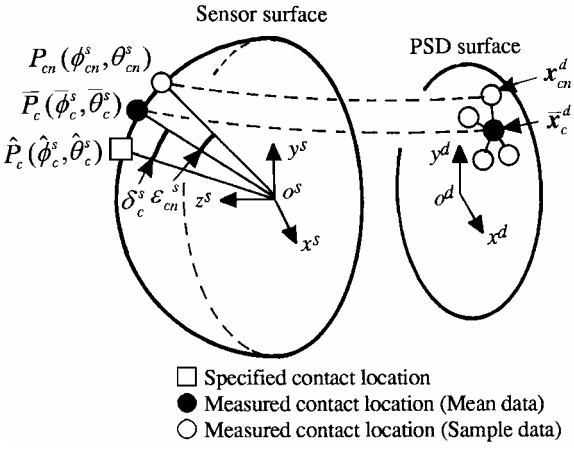

Fig. 5 Accuracy of measurement for static contacts

Fig. 6 Experimental setup for static contacts

found that the contact location of the object was successfully measured by the developed tactile sensor.

Figure 8 shows the error angle δ_c^s between the mean measured contact location $\overline{P}_c$ and the specified contact location $\hat{P}_c$ for the 25 contact locations shown in Fig. 7. The error angle varies from angle $\hat{\theta}_c^s$, namely the distance of the specified contact location from the pole of the sensor, and every plot corresponds to $\hat{\phi}_c^s$=0, 60, 120, 180, 240, 300° respectively.

When the object contacts the peripheral area of the sensor, the error angle increases to about 6° which corresponds to a displacement of 1.7mm on the sensor surface.

Regarding the reason for the error angle shown in Fig. 7 and 8, we suppose that the optical fibers composing the FOP are not completely allocated uniformly and the optical coupling between the PSD and the sensor surface is distorted from Eqs. (3)-(4). Therefore, the error angle can be reduced by improving the present signal processing to compensate for the distortion of the FOP.

Next, the repeatable accuracy of the tactile sensor was experimentally evaluated. Figure 9 shows the deviation of 20 measured contact locations for three specified contact locations ($\hat{\phi}_c^s$=180°, $\hat{\theta}_c^s$=0, 30,

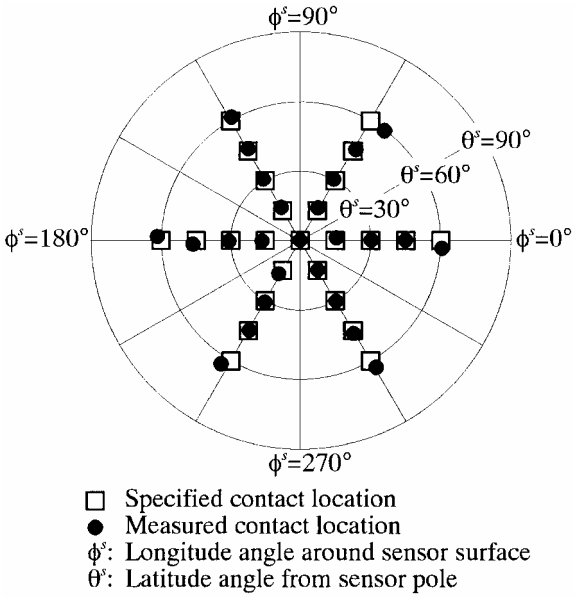

Fig. 7 Sensory output for static contacts

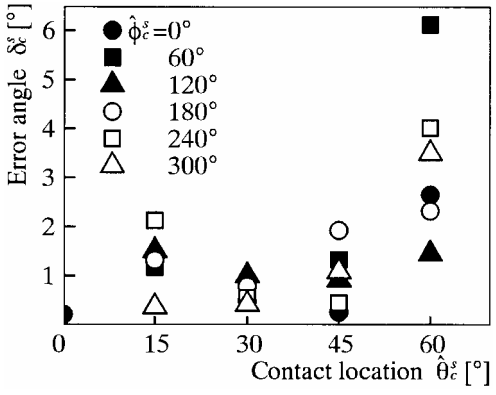

Fig. 8 Error angle of contact measurement

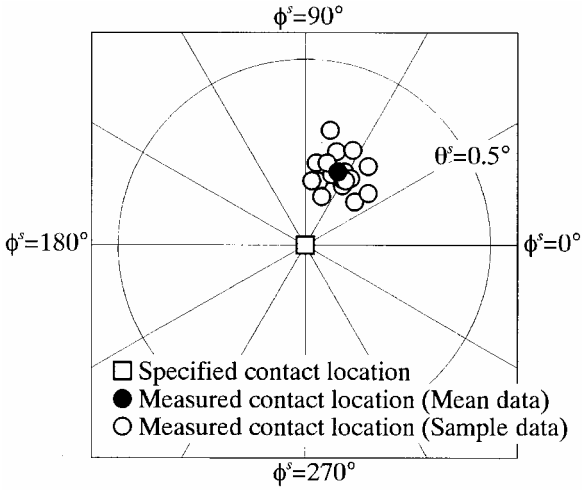

(a) Contact location: $\hat{\theta}_c^s$=0°

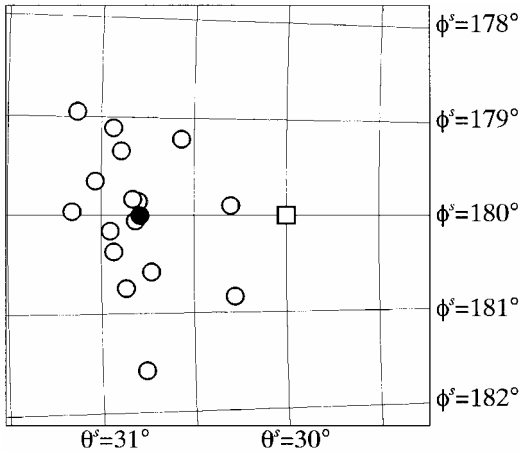

(b) Contact location: $\hat{\phi}_c^s$=180°, $\hat{\theta}_c^s$=30°

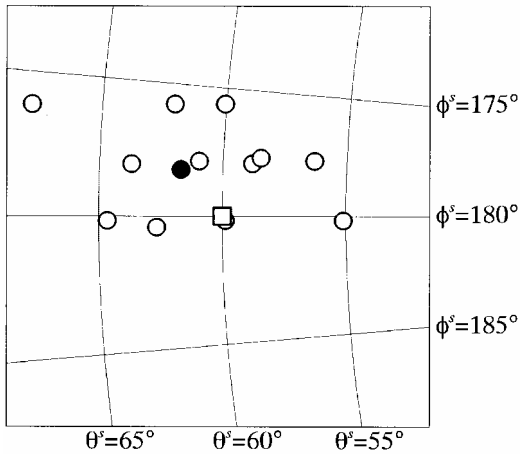

(c) Contact location: $\hat{\phi}_c^s$=180°, $\hat{\theta}_c^s$=60°

Fig. 9 Distribution of sample data for contact measurement

60°). As in Fig. 7, the specified contact location $\hat{P}_c$ is represented by □, the mean measured contact location $\overline{P}_c$ by ● and every measured contact location P_{cn} by ○ in the $\phi^s\theta^s$ polar coordinate system. Figure 10 shows the mean deviation $\overline{\varepsilon}_c^s$ derived by Eqs. (13)-(14) for 25 contact locations varying from the specified contact location $\hat{\phi}_c^s$, $\hat{\theta}_c^s$.

According to experimental results shown in Fig. 9, 10, the mean deviation increases as the object contacts the peripheral area of the sensor surface. However, when the contact location $\hat{\theta}_c^s$ is within 45° from the pole of the sensor, the mean deviation is less than 1.5° (0.4mm on the sensor surface), and that is adequate repeatable accuracy.

The increase of the mean deviation at the peripheral area of the sensor surface occurs because the scattered light is not led well to the PSD through the FOP. As shown in Fig. 2 (b), the FOP in the sensor has a hemispherical larger end that faces the waveguide and a flat smaller end that faces the PSD. Therefore, the optical fibers in the FOP are bent more in the outer part. On the other hand, when the curvature of the optical fiber increases, the scattered light cannot reach the PSD because the angle of incidence to the fiber exceeds the critical angle and total internal reflection is not maintained. For this reason, when the object contacted at the peripheral area of the sensor far from its pole, the intensity of the scattered light led to the PSD decreases and this results in degraded accuracy or loss of the sensing capability. Thus, the design of the FOP needs to account for the curvature of the fibers and be minimized to achieve a tactile sensor that provides accuracy over a wide area.

6.3 Evaluation of tactile sensor for dynamic contact

When the tactile sensor is installed in the fingertip of a robotic hand for detecting tactile information while grasping and manipulating, the contact condition changes dynamically. For practical application, the response of the developed tactile sensor to dynamic changes of the contact was experimentally evaluated.

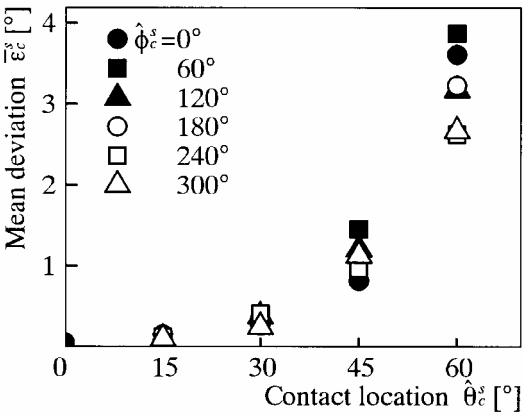

Fig. 10 Mean deviation of contact measurement

The object is intermittently contacted on the sensor using a slider-crank mechanism driven by a speed-controllable motor. A total of four PSD outputs $\Delta v_{x1} + \Delta v_{y1} + \Delta v_{x2} + \Delta v_{y2}$ is recorded during the dynamic contacts. Also the pulse from the photo-interrupter synchronized with the motion of the object is recorded.

Figure 11 shows the output of the PSD and the output of the photo-interrupter for monitoring the motion of the object when the object contacts the sensor during two different periods and intermittent frequencies, 0.25s, 0.88Hz and 0.078s, 3.2Hz. At the beginning of the contact, the elastic cover is depressed by the object and approaches the waveguide. At this moment, the output of the PSD increases slightly, although the cover has not yet contacted the waveguide. This is because part of the light leaks from the waveguide and illuminates the inner surface of the cover. When the cover depressed by the object approaches the waveguide, much of the reflected light at the inner surface of the cover reaches the PSD. Therefore, the output of the PSD increases even if the cover does not actually make contact with the waveguide at that

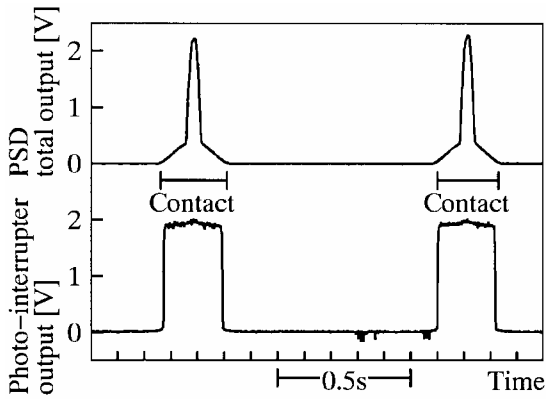

(a) Contact period: 0.25s, Intermittent frequency: 0.88Hz

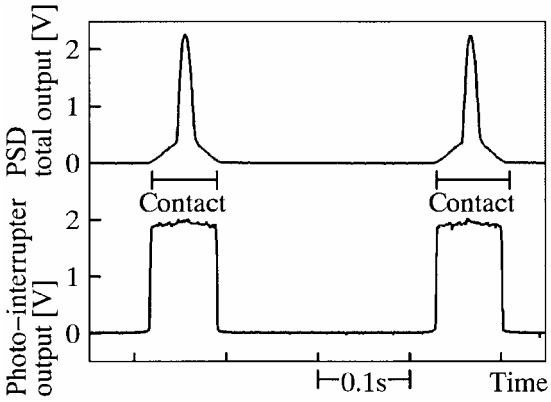

(b) Contact period: 0.078s, Intermittent frequency: 3.2Hz

Fig. 11 Dynamic response of sensor to intermittent contacts

time. Subsequently, when the cover contacts the waveguide, intense scattered light occurs and the peak of the PSD output is observed.

By adjusting the time scale, the transient of the output of the PSD is quite similar in form, whether the contact period is long as shown in Fig. 11 (a), or short as in Fig. 11 (b). This means that the developed tactile sensor responds without significant delay to intermittent contacts with durations as short as 0.078s, the shortest contact period that the present experimental facility can produce. The reason for this quick response is that the silicone rubber composing the cover provides considerable elasticity for deformation and does not stick to the waveguide. Furthermore, the air caught between the cover and the waveguide produces a restoring force which tends to maintain the hemispherical form of the cover when it is depressed.

7. Conclusions

In summary, the following conclusions are reported concerning the development and the evaluation of a finger-shaped tactile sensor:

1. A finger-shaped tactile sensor using a hemispherical optical waveguide capable of detecting the contact location and surface normal of the contacted object was developed.
2. Through the integration of the components, the miniaturization of the sensor was achieved (diameter: 32mm). Also a fast signal processing algorithm for the sensor (processing time: 1.5ms) was developed.
3. The error angle in the contact location measurement increases for contacts at the peripheral area of the sensor (maximally about 6°). However, the mean deviation is less than 1.5° when the contact location is within 45° from the pole of the sensor.
4. The tactile sensor responds without significant delay for intermittent contacts as short as 0.078s.

The developed tactile sensor uses a PSD capable of measuring the location of the optical input instantly. This facilitates simple and fast signal processing. However, the sensor cannot detect multiple contacts separately, since the PSD detects the location of their centroid. This can be resolved by using an image sensor and a high-speed image processor which could simultaneously measure the location of every optical input. Such improvements are under investigation together with further miniaturization of the sensor.

References

[1] Begej, S., Planar and Finger-shaped Optical Tactile Sensors for Robotic Applications, IEEE Journal of Robotics and Automation, vol. 4. no. 5, pp. 472-484, 1988.

[2] Dario, P. and G. Buttazzo, An Anthropomorphic Robot Finger for Investigating Artificial Tactile Perception, Int. Journal of Robotics Research, vol. 6, no. 3, pp. 25-48, 1987.

[3] Fearing, R. S., Tactile Sensing Mechanisms, Int. Journal of Robotics Research, vol. 9, no. 3, pp. 3-23, 1990.

[4] Kerr, J. and B. Roth, Analysis of Multifingered Hands, Int. Journal of Robotics Research, vol. 4, no. 4, pp. 3-17, 1986.

[5] Kolesar, E. S. and C. S. Dyson, Object Imaging with a Piezoelectric Robotic Tactile Sensor, Journal of Microelectromechanical Systems, vol. 4, no. 2, pp. 87-96, 1995.

[6] Nakao, N., M. Kaneko, N. Suzuki and K. Tanie, A Finger Shaped Tactile Sensor Using an Optical Waveguide, Proc. of IEEE Industrial Electronics Society, pp. 300-305, 1990.

[7] Nguyen, V., Constructing Stable Grasps, Int. Journal of Robotics Research, vol. 8, no. 1, pp. 26-37, 1989.

[8] Purbrick, J. A., A Force Transducer Employing Conductive Silicone Rubber, Proc. of Conf. on Robot Vision and Sensory Controls, pp. 73-80, 1981.

[9] Salisbury, J. K. and J. J. Craig, Articulated Hands: Force Control and Kinematic Issues, Int. Journal of Robotics Research, vol. 1, no. 1, pp. 4-17, 1982.

[10] Tanie, K., K. Komoriya, M. Kaneko, S. Tachi and A. Fujikawa, A High Resolution Tactile Sensor, Proc. of Conf. on Robot Vision and Sensory Controls, pp. 251-260, 1984

[11] Vranish, J. M., Magnetoresistive Skin for Robots, Proc. of Conf. on Robot Vision and Sensory Controls, pp. 269-284, 1984.

Hitoshi Maekawa received B. E. (1986), M. E. (1988) and Ph. D. (1997) degrees in control engineering from the Tokyo Institute of Technology, Japan. He joined the Mechanical Engineering Laboratory, Ministry of International Trade and Industry, in 1988. From 1997 to 1998, he was a postdoctoral visiting researcher at the University of Utah, USA. Since 2001, he has been a senior researcher of the Collaborative Research Team of Welfare Technology, National Institute of Advanced Industrial Science and Technology. His research interests include the control of the dexterous multifingered hand, development and application of the finger-shaped tactile sensor, and material handling technology in the microfactory.

Kazuo Tanie received B. E. (1969), M. E. (1971) and Dr. Eng. (1980) degrees in mechanical engineering from Waseda University, Japan. He joined the Mechanical Engineering Laboratory, Ministry of International Trade and Industry (MITI) in 1971 and was the director of Department of Robotics between April 1997 and March 2001. With

reform of MITI's laboratories, he has been with the National Institute of Advanced Industrial Science and Technology since April 2001, and is now the director of the Intelligent Systems Institute. Currently, he is also an adjunctive professor of the University of Tsukuba, and a visiting professor of Waseda University. His research interests include virtual reality and its application to tele-robotics, design and control of dexterous robotic arms and multifingered hands, power assist systems for rehabilitation, and macro-micro robotic teleoperation. He received the Engelberger Robotics Award in 2001. He has published more than 250 journal and conference papers.

Makoto Kaneko received B.S. (1976) degree in mechanical engineering from Kyushu Institute of Technology, Japan, M.S. (1978) and Ph. D. (1981) degrees in mechanical engineering from the University of Tokyo, Japan. From 1981 to 1990, he was a researcher at the Mechanical Engineering Laboratory, Ministry of International Trade and Industry. From 1988 to 1989, he was a postdoctoral scholar at Technical University of Darmstadt (TUD), Germany. From 1990 to 1993, he was an associate professor with Computer Science and System Engineering at Kyushu Institute of Technology. Since October 1993, he has been a professor of Industrial Engineering Department at Hiroshima University. His research interests are in tactile-based active sensing, grasping strategy, super-high speed manipulation, sensor applications, and welfare robotics. He received the Humboldt Research Award (1997), the Best Manipulation Paper Award (2000) in IEEE ICRA, and the Outstanding Paper Award (2001) in IEEE ISATP.

Natsuo Suzuki received B. S. (1978), M. S. (1980) and Ph. D. (1984) degrees in precision engineering from the University of Tokyo, Japan. From 1984 to 1987, he was an assistant at Tokyo Denki University. From 1987 to 1991, he worked at Mechanical Engineering Laboratory, Ministry of International Trade and Industry. Since 1991, he has been an associate professor of Mechanical Engineering Division at Tamagawa University. His current research interests include mechatronic and robotic devices, nonlinear dynamics and chaos.

Chiyoharu Horiguchi graduated from Short Term Department of Chiba University, Japan in 1972. He joined Hamamatsu Television K. K. (Hamamatsu Photonics K. K.) in 1972 and now an assistant department manager of Department 33. His research interests include the optical sensing technology and development of a 3D measuring system.

Takeo Sugawara received B. Sc. (1972) degree from Yamagata University, Japan. He joined Hamamatsu Television K. K. (Hamamatsu Photonics K. K.) in 1972. He has been involved in the development of a micro channel plate (MCP) and a fiber optics plate (FOP).

Translated from Trans. of the SICE, Vol. 30, No. 5, 499/508 (1994)